WILEY InterScience® DISCOVER SOMETHING GREAT

PROTEINS STRUCTURE ■ FUNCTION ■ BIOINFORMATICS

Evaluation of docking programs for predicting binding of Golgi α-mannosidase II inhibitors: A comparison with crystallography

Pablo Englebienne,[1] Hélène Fiaux,[1,2] Douglas A. Kuntz,[3] Christopher R. Corbeil,[1] Sandrine Gerber-Lemaire,[2] David R. Rose,[3] and Nicolas Moitessier[1]*

[1] Department of Chemistry, McGill University, Montréal, Québec H3A 2K6, Canada

[2] Institute of Chemical Sciences and Engineering, Ecole Polytechnique Fédérale de Lausanne (EPFL), BCH, CH-1015 Lausanne, Switzerland

[3] Ontario Cancer Institute and Department of Medical Biophysics, University of Toronto, Toronto, Ontario M5G 1L7, Canada

ABSTRACT

Golgi α-mannosidase II (GMII), a zinc-dependent glycosyl hydrolase, is a promising target for drug development in anti-tumor therapies. Using X-ray crystallography, we have determined the structure of* Drosophila melanogaster *GMII (dGMII) complexed with three different inhibitors exhibiting IC_{50}'s ranging from 80 to 1000 μM. These structures, along with those of seven other available dGMII/inhibitor complexes, were then used as a basis for the evaluation of seven docking programs (GOLD, Glide, FlexX, AutoDock, eHiTS, LigandFit, and FITTED). We found that small inhibitors could be accurately docked by most of the software, while docking of larger compounds (i.e., those with extended aromatic cycles or long aliphatic chains) was more problematic. Overall, Glide provided the best docking results, with the most accurately predicted binding around the active site zinc atom. Further evaluation of Glide's performance revealed its ability to extract active compounds from a benchmark library of decoys.

Proteins 2007; 69:160–176.

***Key words:* Glide; FITTED; virtual screening; scoring; crystal structure.**

INTRODUCTION

Glycoproteins and glycolipids are major components of the outer surface of mammalian cells and the majority of cell surface and secreted proteins of eukaryotes are glycosylated. The carbohydrates are commonly bound to an asparagine residue within the sequence Asn-X-Ser (or Thr) through an *N*-glycosidic linkage.[1] The glycosylation process corresponds to a post-translational modification involving a large panel of specific glycosidases and glycosyltransferases, and is responsible for proper processing of proteins. The biosynthesis of Asn-linked glycoproteins[2–4] starts in the endoplasmic reticulum then progresses in the Golgi apparatus to produce the mature glycosylated structure on the nascent protein.[5,6] This second step is highly dependent on species, tissues and cells, thus resulting in the diverse nature of the final branched oligosaccharides. The Golgi α-mannosidase II (GMII) is responsible for the specific trimming of two mannose residues from the branched $GlcNAcMan_5GlcNAc_2$ mannose intermediate, with retention of sugar anomeric configuration, and is therefore a key enzyme of the Golgi processing pathway.

In various tumor cells, the distribution of cell surface *N*-linked oligosaccharides is altered and correlates with disease progression, metastasis and poor prognosis.[7–10] GMII has consequently been viewed as a potential target in the development of new anti-cancer therapies. In clinical trials, swainsonine, a natural inhibitor of GMII featuring a 4-amino-4-deoxy-mannofuranoside unit[11,12] has been shown to reduce certain tumors and hematological dysfunctions.[13,14] However, the co-inhibition of lysosomal mannosidases prevents further development of this compound towards medicinal treatments. It is thus highly important to find highly specific inhibitors of GMII that would exhibit anti-cancer activity.

In an ideal scenario, medicinal chemists use three-dimensional structures of the various protein targets to design potent and selective inhibitors. In fact, docking studies performed on various mannosidases would aid in the computational evaluation of the selectivity of the inhibitors. Unfortunately, mammalian mannosidases

Grant sponsors: Swiss National Science Foundation; Grant number: N°200020-107532/1; Virochem Pharma, Canadian Foundation for Innovation (New Opportunities Fund), NSERC (discovery grant), Canadian Institutes for Health Research.
*Correspondence to: Nicolas Moitessier, Department of Chemistry, McGill University, 801 Sherbrooke Street W., Montréal, Québec H3A 2K6, Canada. E-mail: nicolas.moitessier@mcgill.ca
Received 10 November 2006; Revised 15 February 2007; Accepted 22 February 2007
Published online 7 June 2007 in Wiley InterScience (www.interscience.wiley.com). DOI: 10.1002/prot.21479

are difficult to purify in suitable quantities and to date only a single structure of bovine lysosomal mannosidase is available with a suboptimal resolution of 2.70 Å, which hinders the possibility of performing accurate docking experiments on it.

Jack bean α-mannosidase was first found to be a readily available and reliable model enzyme for assaying inhibition of mammalian GMII, however its crystal structure and primary sequence has not yet been determined.[15] More recently, *Drosophila melanogaster* GMII (dGMII), which displays high sequence identity with human GMII (hGMII), 40% identity and 70% homology, was used as a valid model of the structural and functional features of the mammalian enzyme.[16–18] In particular, it has been shown that the exposed residues in the active site cavity are almost completely conserved between hGMII and dGMII.[17] As a consequence, the latter was used in place of hGMII in various crystallographic studies and has recently provided a series of crystal structures of GMII:inhibitor complexes.[19] This newly available structural data could now be the starting point for the structure-based design of potentially active and selective GMII inhibitors. For this purpose, we naturally turned our attention to the available computational structure-based drug design methods.

For the last two decades, computational methods for structure-based drug design have evolved significantly. Their increasing accuracy has been followed with growing interest by the pharmaceutical industry. Among these methods, docking techniques have been extensively investigated and exploited in medicinal chemistry projects. Unfortunately, no universal method (i.e., applicable to any protein target) has been discovered and the choice of the software has to be done wisely.[20] While the accuracy of existing methods is increasing, remaining limitations have been identified. The flexibility of the enzyme and the presence of key water molecules are major issues yet to be addressed.[21,22] To account for the induced-fit of the protein upon binding of a ligand, several strategies have been proposed.[23]

We report herein our efforts in the structural determination of dGMII:inhibitor complexes and their use in docking studies. In particular, three new structures of dGMII:inhibitor complexes are presented. The present work had two main goals, the additional validation of our recently developed software FITTED and the identification of accurate software for designing and screening potential GMII inhibitors. Thus, a large section of this report will be devoted to a comparative study of the most accurate docking programs, namely Glide,[24] GOLD,[25] FlexX,[26] LigandFit,[27] eHiTS,[28] AutoDock[29] and FITTED[30] in combination with a large panel of scoring functions. This study was not intended to fully evaluate these docking programs but to find the best one in the context of mannosidase inhibition. A last section will describe the assessment of the accuracy of Glide in a virtual screening study.

MATERIALS AND METHODS

Enzyme assays and crystallography

Measurement of inhibition, crystallization, data collection, and structural refinement were carried out essentially as outlined by Kuntz et al.[31] with the exceptions noted below. Crystals of dGMII were grown overnight, washed with phosphate buffered reservoir solution (as per Shah et al.[32]) and soaked with 10 m*M* **8** and **9** for at least 3 h. In the case of **10**, crystals were soaked in Tris-buffered reservoir solution without phosphate washing. Data were collected on Beamline 191D at the Advanced Photon Source for crystals of **8** and **9** and at Beamline A1 at the Cornell High Energy Synchrotron Source for **10**. 400 frames with 0.5° oscillation/frame were collected. To obtain a data set with good completeness, data on two crystals of **9** were collected and the data merged with Scalepack.

Preparation of structures for docking

The structures of the dGMII complexes were retrieved from the Protein Data Bank (PDB codes: 1HWW, 1HXK, 1PS3, 1R33, 1R34, 1TQS, 1TQT, as well as the newly determined 2F18, 2F1A, 2F1B presented here) and prepared using Maestro 7.0[33] from Schrödinger as follows. Water molecules were removed and the resulting proteins were aligned based on the α-carbon trace. Hydrogen atoms were added to both proteins and ligands, and bonds to the zinc atom were broken. The atom types and partial charges were first assigned automatically. Charges of the catalytic site residues were corrected following a DFT calculation at the B3LYP/6-31G** level of theory (Jaguar 6.0[34]) on a truncated site consisting of His90, His471, Asp92, Asp204 and Zn; Mulliken populations were considered as the source of the charges. These charges were assigned at different stages depending on the docking software used. Appropriate zinc atom van der Waals parameters were obtained from the literature[35] and implemented in each program requiring these parameters. The structures of the ligands were optimized through energy minimization (Tripos force field) prior to the docking (MLS, minimized ligand structures); the original crystal structure (CLS, crystal-derived ligand structures) conformations were kept for RMSD measurements.

Glide

Neutral zones (as defined in Glide) of 10–20 Å around the ligands were first defined and the inhibitor/proteins were refined using the local optimization procedure proposed in Glide. The zinc parameters were added to the OPLS2003 force field definition and specific charges were assigned to the catalytic residues and zinc atom. The rest of the protein and the ligands were assigned Macromodel/

OPLS2003 charges and atom types. Grids were prepared for each protein with the exact same center and a size of 40 Å. A constraint that forced the interaction with the metal ion was included. A specific keyword (CMAE) was employed for the DFT-derived partial charges (see above) to be maintained during the grid preparation. Preparation, refinement and grid calculation took about 4 h per protein on an SGI R16K. The ligands were minimized using the OPLS2003 forcefield and submitted to Glide for docking. To ensure convergence, an exhaustive search was secured by using search parameters set to their maximum values and a set of 25 runs. This exhaustive search led to the docking of the 10 inhibitors on a single receptor in an average time of 44 min on an SGI R16K. The following parameters were used: ligvdwscale factor 1.0; maxkeep 50,000; maxconf 10,000; nreport 5000; maxref 4000; scorecut 100. A specific keyword (reference) was needed to report the RMSD.

Glide VS

Default parameters were used to dock with Glide; the time-consuming exhaustive search described above was discarded in order to better simulate a realistic virtual screening study. The protein target 1PS3 was used as prepared for the Glide docking described above. Ligands **11–17** were prepared for docking as described in Preparation of structures for docking.

FlexX

The input structures were prepared using the Sybyl 7.0 interface.[36] Binding sites based on proteins truncated at 7.0 Å around the inhibitors were used; ligand MLS structures were used as recommended in the FlexX User Manual. The RIGID_RING mode was selected in order to keep the input conformation as the sole ring conformation (as for Glide and AutoDock). The torsion-standard.dat library of torsions was used. All the other default parameters for the various incremental construction stages or for the input file setup were used. An additional metal pharmacophore-filter using the FlexX-Pharm module was used. All the successful poses were kept for further analysis. Rescoring with the scoring functions implemented in CScore of both the nonrelaxed (FlexX output) and relaxed (Tripos force field) docked poses was performed on a receptor featuring the free coordination sites of the Zn atom as dummy atoms (Tripos atom type "Du").

AutoDock

The AutoDock Tool interface was used to prepare the ligands and the proteins. Kollman charges and solvation parameters were assigned to the protein. The created pdbqs proteins files were modified to account for the presence of a metal (called M) and the calculated charges for the catalytic site residues and the zinc ion. Grids of identical size and center as for the Glide study were computed. Gasteiger-Marsili charges were assigned to the inhibitors whenever possible.[37] Otherwise, when nonparameterized groups (e.g., sulfur cation) were present, partial charges were computed using the MOPAC semi-empirical method (Mulliken charges). Both the CLS and MLS were used as input. Twenty-five runs with a maximum of 1,000,000 energy evaluations and a population size of 100 individuals were performed. The same calculations were also done with a maximum of 5,000,000 energy evaluations and a population of 200 individuals but did not show any improvement. This last set of computations indicates a good convergence using a maximum of 1,000,000 energy evaluations and a population size of 100 individuals. The default parameters for the Solis and Wets optimization and the genetic operators were used.

eHiTS

No interface is provided with eHiTS. The protein input structures were given as pdb files and the ligands as mol2 files. The receptor was truncated keeping any residue with at least one atom within 7.0 Å from any of the inhibitors. The CLS and MLS were alternatively used. The docking was performed using the default parameters for the docking (fragment docking, graph matching algorithm, and pose optimization) and scoring. The highest accuracy was selected.

GOLD

The protein and ligand (MLS) mol2 files prepared previously were used for this study. Most of the optimized parameters were set as defaults (population size of 100 individuals, five islands, niche size of two, and a selection pressure of 1.1). However, in order to ensure an exhaustive search for each ligand, the following parameters were used: 200,000 as maximum operations allowed and a binding site defined using a radius of 18 Å. A substructure constraint (alcohol functional group within 2.5 Å from the zinc atom with a spring constant of 5.0 kcal/Å^2) was also used in a set of runs. The docking terminated when the top three solutions were within 1.0 Å, otherwise 25 runs were carried out. ChemScore and GoldScore scoring functions were used alternatively. Although the metal coordination can be automatically determined, we overruled the automatic definition and set two possible metal coordination geometries (trigonal bipyramidal and octahedral).

LigandFit

The protein and ligand (MLS) structures prepared previously were loaded on Cerius2.[38] Self-docking with the zinc atom defined as a "feature" was first attempted with the three scoring functions (PLP, CFF, Dreiding); cross-

DOI 10.1002/prot

docking was carried out only with PLP. Default parameters were used.

FITTED 1.0

The protein and ligands were processed using ProCESS and SMART, two modules in FITTED.[30] Population sizes of 100 individuals were used and a maximum of 100 generations were carried out. All other default parameters were used as defined elsewhere.[30] To avoid a strong bias of the docking, a sphere as large as 6.0 Å centered on the zinc atom was used to orient the metal-binding moieties in the docking.

RESULTS AND DISCUSSION

Docking data set

Seven structures of dGMII:inhibitor complexes were selected from available crystal structures in the Protein Data Bank (PDB)[39] and added to the three described below. Structures with ligands that are not competitive inhibitors or structures with resolution worse than 2.0 Å were discarded. Ligands **1–7** (Table I) were selected to represent a wide range of activity against dGMII. The seven dGMII:inhibitor complexes were imported from the Protein Data Bank: 1HWW (swainsonine),[17] 1HXK (1-deoxymannojirimycin),[17] 1PS3 (kifunensine),[32] 1R33,[40] 1R34,[40] 1TQS (salacinol),[31] and 1TQT.[31] We also included in this study three polyfunctionalized pyrrolidine derivatives (**8–10**) related to the family of α-mannosidase inhibitors developed by Vogel and co-workers[41–43] which were co-crystallized in the active site of dGMII (2F18, 2F1A, 2F1B). The latter inhibitors could be described as consisting of a pyrrolidine head coupled to a phenylglycinol tail.

Crystallography

We report here the information retrieved from the analysis of the crystal structures of dGMII complexed with inhibitors **8**, **9,** and **10**. Resolution of the synchrotron collected data was 1.30–1.45 Å and R_{free} was 18–19% for the three structures. Detailed data collection and refinement statistics are presented in Table II. Figure 1 shows the quality of the electron density around the bound inhibitors. The density for inhibitors **8** and **10** was much cleaner in the "tail" region of the aromatic ring than the similar region of inhibitor **9**. For **9**, the electron density of the aromatic ring was only visible when the contour levels of the maps were lowered significantly. The average temperature factors for the aromatic groups of **8** and **10** were 16 and 17.6, respectively, while for **9**, it was 32.5. This indicated that this region of **9** was in an unfavorable location, and might be oscillating between numbers of positions so that it did not show up clearly in the electron density map. This lack of good density correlated well with the poorer inhibitory activity for **9** (IC_{50} = 720 μ*M* vs. IC_{50} = 80 μ*M* for **8**). The configuration of the phenylglycinol residue was thus a determinant of the recognition process.

The binding of the highly active inhibitor **8** in the active site of dGMII is illustrated in Figure 2 and a list of interactions between the three inhibitors and the protein where the interaction distance was less than 3.2 Å is given in Table III. For comparison, the interaction distances with swainsonine **1** (IC_{50} = 17 n*M*) are also indicated. These distances were derived from a high resolution (1.30 Å) dGMII:**1** co-crystal structure.[17] The major changes between the three pyrrolidine-based inhibitors occurred in the interaction with the terminal hydroxyl group (OH-9). The importance of the two hydroxyl groups on the pyrrolidine ring was clear. There were tight interactions between the hydroxyl moieties and the active site zinc as well as interactions with His90, Asp92, Asp204, His471, and Asp472. An unusual feature of the inhibitors presented in this article was that there was no hydroxyl group occupying the space between Asp472 OD1 and Tyr727 OH (Figure 2). In all the structures that we have previously examined there has been a hydroxyl group on the bound compound sitting between Asp472 OD1 and Tyr727 OH. In the case of phosphate-washed crystals where no compound was bound in the active site, the position was occupied by a water molecule. (Kuntz DA, unpublished results) As a result of this absence of hydroxyl group, the Tyr727 OH was shifted about 0.6 Å towards the Asp472 OD1. Other interactions with the inhibitors were also seen, in particular with N7 in the "tail" region. Trp95 made two important interactions with the inhibitors. There was a T-shaped interaction between the aromatic ring in the inhibitor and the indole in the tryptophan side-chain, the two planes being at near right angles of each other. Trp95 also made stacking hydrophobic interactions with the pyrrolidine ring, a common feature of GMII complexes.[17]

In the dGMII:**8** complex, the terminal oxygen (O9) made numerous hydrogen bonds. It was 2.7 Å from Asp340 OD1, 2.8 Å from a water molecule, 3.3 Å from Tyr269 OH, and 3.5 Å from Asp341 OD1. An almost identical bonding pattern was seen for inhibitor **10**, although the interaction distances were slightly longer. The oxygen (O9) was 2.7 Å from Asp340 OD1, 2.8 Å from a water molecule, 3.5 Å from Tyr269 OH, and 3.7 Å from Asp341 OD1. Because of the different stereochemistry of the inhibitor **9**, the O9 oxygen sat in a different location and was now 4.8 Å from Asp340 OD1 and 4.5 Å from Asp341 OD1. Nevertheless, there were still interactions with Tyr269 and two water molecules (Table III).

Inhibitors **8** and **10** exhibited virtually identical binding modes in the active site of dGMII (Fig. 3), despite the additional methyl group on the pyrrolidine ring in **10** (labeled C21 in the PDB file). In the protein, however,

Table I
Selection of Structures of α-Mannosidase/Inhibitor complexes

Compound	IC_{50} (μM)	PDB code	Resolution (Å)	R/R_{free}	Inhibitor structure
1 (Swainsonine)	0.017[16]	1HWW[17]	1.87	0.18/0.21	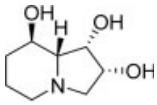
2 (DMNJ)	400[19]	1HXK[17]	1.50	0.20/0.22	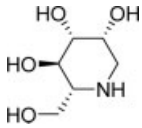
3 (Kifunensine)	5200[a][41]	1PS3[41]	1.80	0.20/0.22	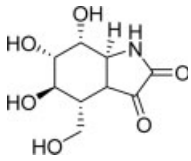
4	70[42]	1R33[42]	1.80	0.16/0.19	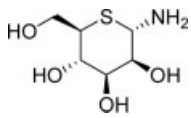
5	900[42]	1R34[42]	1.95	0.15/0.20	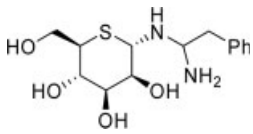
6 (Salacinol)	7500[43]	1TQS[43]	1.30	0.16/0.18	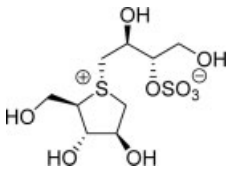
7	7500[43]	1TQT[43]	1.90	0.15/0.18	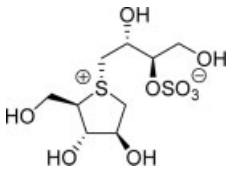
8	80[b]	2F18[b]	1.30	0.17/0.18	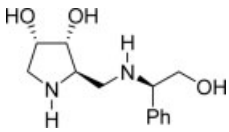
9	720[b]	2F1A[b]	1.45	0.17/0.19	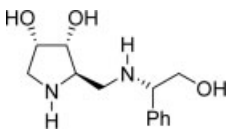
10	1000[b]	2F1B[b]	1.45	0.17/0.19	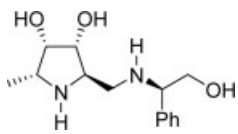

The inhibitory activity (IC_{50}) was measured on dGMII (EC 3.2.1.114) at 37°C, pH = 5.75.
All protein crystal structures correspond to *Drosophila melanogaster* GMII.
[a]K_i value.
[b]This work.

Table II
Data Collection and Structural Refinement Statistics

	Compound		
	8	9	10
PDB code	2F18	2F1A	2F1B
HET symbol	GB1	GB2	GB3
Data Collection			
X-ray Source	APS	APS	CHESS
Cell dimensions (Å)	68.97 × 109.7 ×138.9	68.90 × 109.4 × 138.6	69.43 × 110.6 × 139.9
Data processing (denzo/scalepack)			
Resolution (Å) (overall/hi_res)	30–1.30/1.35–1.30	30–1.45/1.50–1.45	30–1.45/1.48–1.45
Redundancy (overall/hi_res)	10.8/5	12.5/10	3.9/3
I/sigma (overall/hi_res)	39/5.1	18.5/3.7	15/2.8
% Completeness (overall/hi_res)	99.9/99.6	96.3/88.0	95.8/97.7
R merge (overall/hi_res)	0.066/0.35	0.06/0.57	0.066/0.50
Refinement (CNS)			
R_{test}/R_{free}	0.168/0.180	0.168/0.189	0.173/0.194
Amino acids	1014	1015	1014
Alternate conformations	33	29	35
Water molecules	1172	1099	1158
rmsd bonds (Å)	0.019	0.016	0.023
rmsd angles (°)	2.2	1.8	1.9
Average B-factors (Å^2)			
Overall	15.3	20.9	17.6
Protein main chain	12.5	18.0	14.7
Protein side chain	14.9	20.9	17.2
Water	26.0	31.3	28.6
Inhibitor	12.7	25.5	15.0
(MPD,NAG,PO4,Zn)	30.5	38.0	33.0

the active site region was opened up in the structure of **10** compared to the structure of **8**, Phe206 and Tyr727 being pushed away from the inhibitor. The distance between C2 in the inhibitors and CZ of Phe206 was 4.8 Å in the **10**:dGMII complex, while it was 4.3 Å in the **8**:dGMII adduct. The Tyr727 OH was shifted 0.4 Å away from C21. The additional methyl group in **10** was in a position normally occupied by a polar hydroxyl in other inhibitors; the conformational stress put on the enzyme to accommodate its binding might be a reason for the poorer affinity of **10** relative to **8** (IC_{50} = 1000 μ*M* vs. IC_{50} = 80 μ*M*).

The position of the aromatic group was similar to that occupied by the ends of the chain of the salacinol analog complexes.[31] An overlay of the crystal structure binding mode of the diastereomer of salacinol (**7**) with **8** is shown in Figure 4(b). Both of these inhibitors exhibited very clear density in their "tail" regions. This suggested that these parts of the inhibitors were occupying a favorable area of the active site space. Nevertheless, a major difference was that the zinc ion was bound to two hydroxyl groups of the inhibitor **8**, but only to one hydroxyl group of the diastereoisomer of salacinol (**7**). This might account for the poor inhibitory properties of **7** in comparison with **8** (IC_{50} = 7.5 m*M* vs. IC_{50} = 80 μ*M*).

The binding modes of **8** and swainsonine (**1**) are compared in Figure 4(b). It was obvious that although the interatomic distances were almost identical (Table III), there was a slight shift in the binding position of **8**. This shift along with the presence of the long and flexible aromatic tail (leading to entropy loss upon binding), the additional ammonium group (high desolvation cost upon binding) as well as the lack of a third hydroxyl interacting with the protein, might account for its weaker inhibitory potency (IC_{50} = 80 μ*M* for **8** vs. IC_{50} = 17 n*M* for **1**).

Docking of GMII inhibitors—general considerations

A close look at the crystal structures revealed challenges for the accurate docking of GMII inhibitors. First, a zinc atom was involved in the catalytic activity of this enzyme and in the strong binding of the selected inhibitors. Second, a few of the active inhibitors featured solvent-exposed moieties that were not specifically interacting with any of the enzyme residues as exemplified by the electron density of compound **9** in Figure 1. Third, there were bound water molecules that made important interactions with the inhibitors (in the case of **8**, at the amino group in the pyrrolidine ring and the O9 oxygen in the tail region). It was therefore expected that docking accuracy would be linked to a proper handling of the zinc ligation and solvation/desolvation by both the conformational sampling engine and the scoring function.

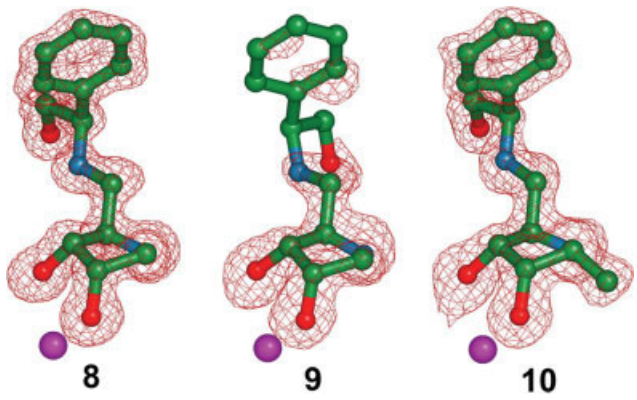

Figure 1

*Electron density representation of the inhibitors **8**, **9** and **10** bound in the active site of dGMII. Maps are simulated annealing omit maps (F_o-F_c) of only the inhibitors contoured at 3.5 σ. For orientation purposes the active site zinc ion is represented as a magenta ball. This figure was generated with PyMOL.*

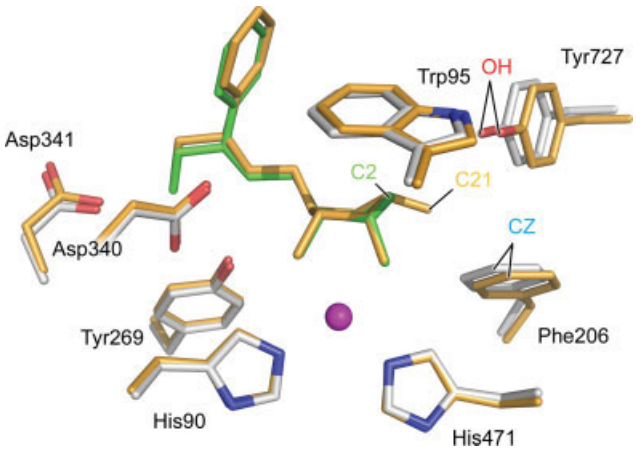

Figure 3

*Comparison of the conformation of the active site residues in the complexes of **8** (ligand green, protein grey) and **10** (ligand and protein orange) with dGMII. The zinc atoms appear as magenta balls. This figure was generated with PyMOL.*

Water molecules were present in some of the complexes; however their locations were not conserved among the different complexes. As it would have been impossible to keep them without biasing the self-docking of an inhibitor to its natural solvated receptor, they were not considered for the present docking study. Ideally, when performing virtual screening or *de novo* design of enzyme inhibitors, water molecules should be properly located or displaced by the docking program, a feature not implemented or in development in most of the available software. To date, only FITTED can move and displace water molecules[30,44] while GOLD can toggle their presence on or off.[25]

After addition of the hydrogen atoms to the crystal structures, the ligands were removed and the proteins were charged and prepared for their use in the subsequent docking study. Special attention was given to the catalytic site including two histidines, two aspartates, and a zinc ion. Although the formal charge of the zinc atom is +2, it was clear that this charge was delocalized onto the chelating residues.[45] The charges for the catalytic site residues and for the zinc atom were derived from density

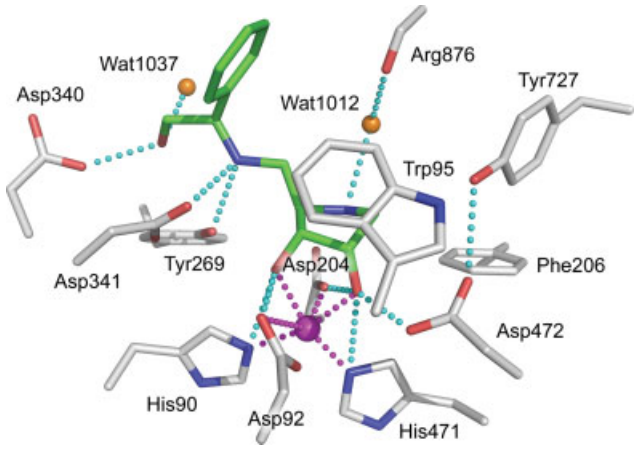

Figure 2

*(**a**) Interaction of **8** with residues in the active site of dGMII. Interactions closer than 3.2 Å are indicated with cyan dotted lines; interactions with the zinc ion are indicated in magenta. Water molecules appear as orange balls. Distances are presented in Table III. This figure was generated with PyMOL.*

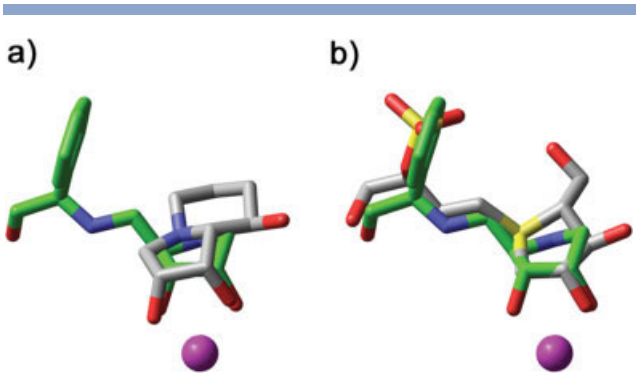

Figure 4

*Overlays of the binding of **8** with (**a**) swainsonine **1** (PDB code 1HWW) and (**b**) the diastereomer of salacinol **7** (PDB code 1TQT). **8** is drawn in green, **7** and **1** are drawn in grey. The active site zinc is represented as a magenta ball.*

DOI 10.1002/prot

Table III
Summary of Interatomic Distances (Å) Between the Inhibitors and dGMII

Zinc interactions				
Compound	**1**	**8**	**9**	**10**
PDB code	1HWW	2F18	2F1A	2F1B
Protein or inhibitor atom	Distance (Å)	Distance (Å)	Distance (Å)	Distance (Å)
H90 NE2	2.10	2.12	2.11	2.14
D92 OD1	2.24	2.13	2.16	2.17
D204 OD1	2.17	2.09	2.08	2.11
H471 NE2	2.09	2.11	2.09	2.13
OH-1 (**1**)/OH-3 (**8**–**10**)	2.20	2.18	2.20	2.20
OH-2 or OH-4	2.13	2.26	2.35	2.31

Protein/ligand interactions								
Compound		**1**		**8**		**9**		**10**
PDB code		1HWW		2F18		2F1A		2F1B
Protein Atom	Atom	Distance (Å)	Atom	Distance (Å)	Atom	Distance (Å)	Atom	Distance (Å)
D92 OD1	OH-1	3.03	OH-3	2.99	OH-3	2.98	OH-3	3.03
	OH-2	2.92	OH-4	3.11	OH-4	3.18	OH-2	3.12
D92 OD2	OH-2	2.54	OH-4	2.69	OH-4	2.61	OH-2	2.59
D204 OD1	OH-1	2.83	OH-3	2.76	OH-3	2.81	OH-3	2.77
	OH-2	2.97	OH-4	2.93	OH-4	2.96	OH-4	2.98
	N-4	2.75	N-1	2.81	N-1	2.88	N-1	2.81
D204 OD2	N-4	3.45	N-1	3.34	N-1	3.36	N-1	3.38
Y269 OH			N-7	3.00	N-7	2.88	N-7	3.14
			OH-9	3.30	OH-9	2.97	OH-9	**3.52**
D340 OD1			OH-9	2.67	OH-9	**4.82**	OH-9	2.66
D341 OD1	OH-8	2.56	OH-9	3.49	OH-9	**4.48**	OH-9	**3.70**
D341 OD2			N-7	2.78	N-7	2.85	N-7	2.80
			OH-4	3.42	OH-4	3.49	OH-4	3.45
D472 OD1			—	—	—	—	—	—
D472 OD2	OH-1	2.60	OH-3	2.49	OH-3	2.46	OH-3	2.59
Y727 OH	OH-8	2.64	—	—	—	—	—	—
WATERS			OH-9	2.78	OH-9	2.63	OH-9	2.78
			N-1	2.91	N-1	2.94	N	2.96

Distances in bold represent distances greater than 3.5 Å, where no significant hydrogen bonding is expected to occur.

functional theory (DFT) calculations of a truncated binding site and used for AutoDock, Glide, LigandFit, and FITTED. The van der Waals parameters for the zinc atom required for both the protein preparation and the docking study were obtained from the literature.[45] For the following studies, the crystal-derived ligand structure (CLS) and/or optimized energy-minimized ligand structure (MLS) were used as input. A comparative study aiming at identifying a program for future virtual screening of drug design could not provide useful results if CLS's were required as input. In a real drug design scenario, one does not know the final pose and would guess an input structure as MLS. As we will describe in the following sections, selection of the input structures has an impact on the accuracy of some of the docking programs.

Docking methods used in this comparative study and parameterization

Many comparative studies discussed in a recent review have shown Glide and GOLD to be amongst the most accurate docking programs.[20] For instance, Rognan and coworkers[46] ranked GOLD, Glide and Surflex as the most accurate docking programs for their set, followed by FlexX. We have previously obtained good results for the docking of zinc-containing enzyme inhibitors with AutoDock.[47,48] In addition, a recent review of eHiTS indicates that this docking program is a new candidate of interest.[49] We decided to assess GOLD, Glide, FlexX, AutoDock, LigandFit, and eHiTS to see which one, if any, would provide accurate docking results for GMII inhibitors. To add to the validation of our own software, the current version of FITTED[30] was also assessed. It is also worth noting that Glide, FlexX (FlexE), AutoDock, and FITTED have versions where flexibility of the protein is accounted for. Induced-fit docking using Glide/Prime relies on a combination of rigid protein docking and homology modeling techniques to construct the backbone and residue side chains.[50] FlexE relies on docking to composite structures,[51] while AutoDock grids can be combined using appropriate weighting schemes into virtual conformational ensembles.[52] The flexibility of the protein/ligand complexes in FITTED relies on the use of chromosomes to describe the whole complexes.[30,53] A section on the use of these functionalities is included in this manuscript.

The assessed programs covered a variety of conformational search methods: genetic algorithms (GOLD, Auto-

Dock, and FITTED), incremental construction (FlexX), rigid fragment docking and linking (eHiTS), Monte Carlo/matching algorithm (LigandFit) and multilevel search (Glide) and a large panel of scoring functions (e.g., ChemScore, GlideScore, GoldScore, F-Score, AutoDock scoring function, PMF, RankScore). Some of the evaluated methods came with an interface that was used to prepare the protein and ligand structure and initial keyword files. However, to obtain the best performance from each docking program, the standalone versions with optimized parameters were used. In addition, although the computation of the atomic root mean square deviations (RMSD) was part of the output of Glide, FlexX, and FITTED, we made our own scripts to compute the RMSD's for the AutoDock and eHiTS studies. The deviations were evaluated using the CLS's as references, taking into account only the coordinates of the heavy atoms but accounting for equivalent atoms that can be exchanged by rotation. One of the main issues addressed is the evaluation of the metal coordination as all the assessed programs treat the metal/ligand interaction differently. Therefore the deviations of the docked ligand structures from the CLS's were also computed for the metal ligation (only for the one or two oxygen atoms bound to the metal center).

As all these programs have been reported, we will describe them succinctly, emphasizing the way they treat binding to metal ions and solvation and their application to GMII.

Glide 3.5[24,54]

Glide uses a funnel-type of approach to search the conformational space and the best poses are scored using GlideScore,[55] a scoring function derived from ChemScore.[56] Among the many terms of this scoring function is a term accounting for metal-ligand interactions. However, this term is restricted to anionic ligands, single atom ligation (we will consider diols) and does not account for the specific geometry of metal–ligand complexes. In the present study, the ligands were neutral, and the metal ligation would therefore be modeled as purely electrostatic. GlideScore also includes a unique solvation term which accounts for solvation of solvent-exposed moieties as well as water molecules captured in hydrophobic protein pockets. Glide also proposes the use of constraints to force specific interactions. The user-defined constraints add an additional filter to the hierarchical filtering. To evaluate the impact of constraints on accuracy, two studies—with and without constraints—were carried out. Unexpectedly, filtering off the poses where no groups were in close proximity to the zinc ion did not significantly increase the accuracy of the binding mode prediction.

FlexX 1.13[26,57,58]/CScore[59]

FlexX is conceptually very different to Glide. Rather than using grids, FlexX models the protein with an all-atom representation of the binding site, and while Glide uses an exhaustive conformational search, FlexX builds up the ligand within the binding site by incremental construction.[59] One similarity between Glide and FlexX is the possibility of using pharmacophore-like constraints to force specific interactions between the ligands and the receptor.[60] Poses that do not satisfy the pharmacophoric constraints are removed. In the present work, we imposed the requirement that at least one zinc-binding atom of the ligand should interact with the zinc ion. The incremental construction algorithm accounts for the geometry of ligand–metal interactions but not for metal coordination geometry.

The poses proposed by FlexX were submitted to rescoring by a panel of four scoring functions implemented in CScore, namely PMF, GoldScore, DockScore, and ChemScore. ChemScore includes a specific (but non-directional) term for metal/ligand binding while there is no specific term for metal/ligand interaction in the FlexX, PMF, GoldScore, and DockScore scoring functions.

AutoDock 3.0[29,61]

The inhibitors, modeled using a united atom representation, are flexibly docked into the grids modeling the proteins by means of a Lamarckian genetic algorithm (LGA). The LGA optimizes the ligand pose to find the local minimum by perturbing the genes of the ligand. The scoring function available with the version 3.0 of this suite of programs does not include any specific term for metal–ligand interaction, the metals being treated as charged spheres with no specific coordination geometry. In contrast to other methods used herein, in the current version (version 4.0 is under validation[62]), no constraint can be specified.

GOLD 3.0[25,63]

GOLD also samples the ligand conformational space using a genetic algorithm (GA). However, in contrast to AutoDock, it uses the atomic description of the protein (or a truncated binding site) and allows for the hydroxyl (Ser, Thr, Tyr) and ammonium (Lys) hydrogen atoms to relax upon ligand docking. A large number of parameters can be optimized to improve the accuracy of the conformational search, although only a few were optimized in the present work according to the observed poses of initial runs (e.g., torsion angle distribution databases, constraints to direct the docking towards the observed binding modes, parameters for the GA, and user-defined scoring functions). Upon docking, GOLD makes use of virtual coordination points (which can be specified by the user) to model the chelation of metals, a potentially very important feature for GMII inhibitor docking. In this study, two possible metal coordination geometries were assessed (trigonal bipyramidal and octahedral). The

 DOI 10.1002/prot

GOLD scoring function (GoldScore) as well as ChemScore do not consider the metal coordination geometry, the metal-ligand interaction strength being only distance dependent. As for Glide and FlexX, GOLD allows for the use of constraints (harmonic constraints) to direct and speed up the docking process.

eHiTS[28,64]

A recent software review revealed the high accuracy of eHiTS for docking small molecules to rigid proteins.[49] This review together with a comparative study from the developers (Reid D, personal communication) prompted us to evaluate eHiTS in the prospect of accurately docking α-mannosidase inhibitors. The conformational search sampling is performed by rigid fragment docking followed by linkage and optimization of the reconstructed ligands. This approach, claimed to be "truly exhaustive," is quite different from the methods used by the other programs described herein. The original scoring function is an empirical scoring function with many terms, including a specific term for angle-dependent metal coordination. However, although angles around the ligand atoms are considered, the metal coordination geometry is not optimized. This piece of software is still under development and only a very few parameters are accessible for modification by the user. While this manuscript was in preparation, a new and more accurate scoring function was implemented but has not been assessed in our study.[65]

LigandFit[27,66]

LigandFit first defines the binding site as a series of grid points used to locate the binding site, defines its shape and further docks the flexible ligands. The docking is performed by generating sets of ligand conformations using a Monte Carlo technique and matching these ligand conformations to the binding site partitions. Three scoring options are available, namely CFF and Dreiding force fields, as well as the PLP scoring function. Neither these two force fields nor PLP include a specific treatment of metal ligation. LigandFit also allows for additional constraints using filters. The LigandFit constraint matches a feature atom such as a polar hydrogen with a complementary ligand atom such as a hydrogen bond acceptor oxygen.

FITTED 1.0[30]

To complete the comparative study, FITTED, a program recently developed in our laboratory has been assessed.[30] FITTED exploits a LGA to model the flexibility of both the ligands and proteins. It also includes a specific function for displaceable water molecules. Unlike AutoDock, FITTED optimizes the ligand pose through a Fletcher-Reeves conjugate gradient minimization.[66] The scoring function (RankScore) does not include any specific term for metal/ligand interactions which are treated as hydrogen bonds.[53] Constraints are implemented in FITTED to direct the binding to a specific atom or group of atoms and will be used to select poses with metal chelation.

Application to the docking of mannosidase inhibitors

The 10 selected weak to strong ligands were docked to the 10 protein structures using each of the assessed programs for a total of 100 docking runs (10 self-docking runs and 90 cross-docking runs) for each program. Thus, Glide/GlideScore, FlexX/FlexXScore, FlexX/PMF, FlexX/GoldScore, FlexX/ChemScore, FlexX/DockScore, AutoDock/AutoDock scoring function, eHiTS/eHiTS scoring function, GOLD/GoldScore, GOLD/ChemScore, LigandFit/PLP, LigandFit/CFF, LigandFit/Dreiding, and FITTED/RankScore were successively assessed. Figure 5 summarizes the collected data.

The FlexX docking engine allowed us to evaluate the generated poses. Thus, when we considered the use of FlexX to dock inhibitors **1**–**10** into GMII, all the docked poses were kept for postdocking analysis and rescoring with four other scoring functions (DockScore,[67] PMF,[68] GoldScore,[25] ChemScore[56]) included in the CScore module of Sybyl. Only the results with the ChemScore scoring function are shown as the other four functions were less accurate. In the present study, a pose with an RMSD below 2.0 Å was generated in only 75% on the cases and was identified by the scoring function in less than 40% of the cases. This revealed that a significant portion of the failures was due to poor conformational sampling and not only to inaccurate scoring.

Within GOLD, GoldScore was found to be marginally better than ChemScore. Interestingly, the use of ChemScore with GOLD and FlexX led to similar results while the enhanced version of ChemScore, GlideScore, led to significantly better accuracy when used in conjunction with Glide. LigandFit was found to be inaccurate when CFF or Dreiding force fields were used to score the generated poses. Unexpectedly, CLS provided significantly better results than MLS with eHiTS. When a simple rotation in space or a change in one torsion angle was applied to the CLS used as input structures, the accuracy dropped.

Glide clearly appeared as the most accurate program in this comparative study. The ligands were docked with RMSD's below 1.0 Å in 40% of the cases and below 2.0 Å in 48%. eHiTS was much less accurate with an accuracy of 28% at 2.0 Å RMSD, while the other five programs showed accuracies ranging from 32% (LigandFit) to nearly 40% (FITTED). We were also pleased to see that the accuracy of FITTED was equivalent to that of Glide at RMSD = 2.5 Å.

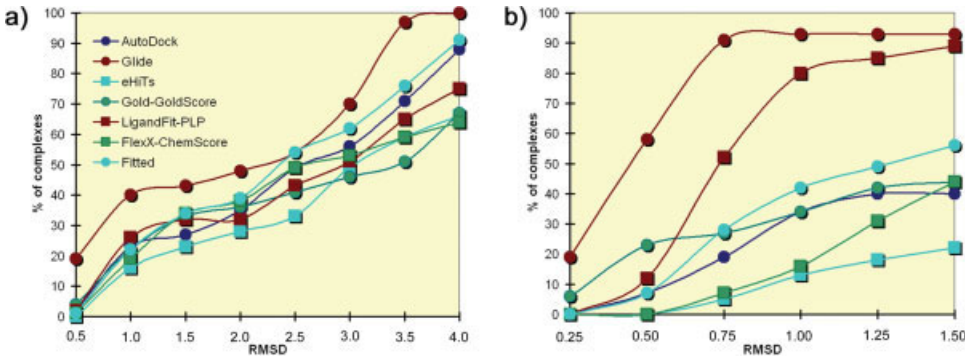

Figure 5

Rigid protein docking. Accuracy for the 7 programs assessed to dock the 10 ligands to the 10 protein structures (self-docking and cross-docking) measured as the RMSD between the docked poses and the crystal structure binding mode for (a) all ligand heavy atoms; (b) metal-binding atoms. [Color figure can be viewed in the online issue, which is available at www.interscience.wiley.com.]

In general, the computed RMSD's indicated better accuracy for the self-docking of the smaller ligands **1**, **2**, **3**, **4**, and **5** with all the programs. For instance, **1**–**5** were docked back to their protein structure (self-docking) with RMSD's below 1.1 Å when the MLS's were used as input with the Glide program. These data are consistent with the results reported in the original Glide publication from Friesner et al. where nearly 50% of the compounds from the testing set were docked back with RMSD's below 1.0 Å.[24] In that same study, about a third of the compounds were docked with RMSD between 1.0–2.0 Å, although in our case ligands **6**–**10** were self-docked with RMSD's higher than 2.5 Å.

To further evaluate the apparent poor docking accuracy observed for ligands **6**–**10**, we inspected the docked and experimentally observed conformations. First, we noticed that the experimentally observed zinc chelation by the diol or alcohol moieties was correctly predicted in almost all of the one hundred complexes when Glide was used, but with poorer accuracy when the other programs were used [Fig. 5(b)]. Second, a close look at the docked structures indicated that the docked pose was for the most part correct in many cases, the main deviation coming from the solvent-exposed moieties and the orientation of the aromatic groups. For instance, compound **8**'s phenyl group was predicted to interact with Arg228 through π interactions, while it was involved in a T-shaped π interaction with Trp95 in the crystal structure (see Fig. 6). In fact, none of the programs predicted the T-shaped interaction between the phenyl ring of **8** and Trp95. This was probably due to the poor description of this type of

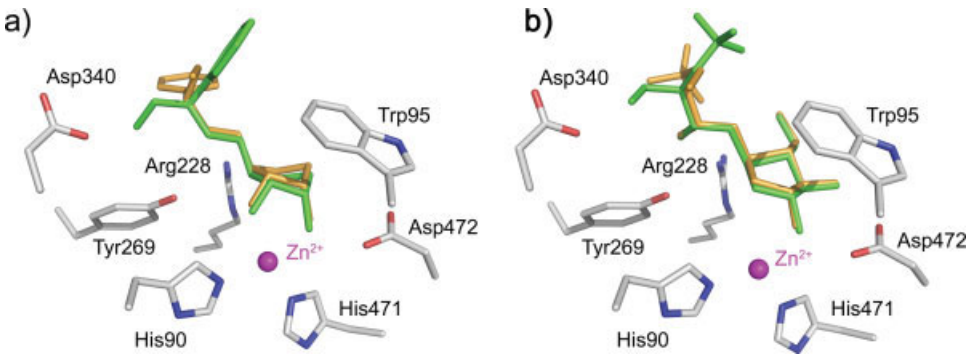

Figure 6

Glide docked vs. *crystallographically observed binding mode of compound **8** (a) and **7** (b). The crystal structure appears in green, the docked structure in orange. This figure was generated with PyMOL. [Color figure can be viewed in the online issue, which is available at www.interscience.wiley.com.]*

DOI 10.1002/prot

interaction by the commonly used scoring functions. Nevertheless, the pyrrolidine ring was perfectly oriented [Fig. 6(a)] in all cases. Similar conclusions were drawn for compounds **9** and **10**. As discussed above, the complex with **9** showed large B-factors for the phenyl ring and a poorly defined electron density map for this solvent-exposed group. The chelation by a single alcohol of **6** and **7** was predicted to occur by Glide [Fig. 6(b)], but the main deviation arose from the positioning of the solvent-exposed sulfate predicted to interact with Tyr267 and/or with Arg228 [Fig. 6(b)]. In the crystal structures, this moiety was solvated while not specifically interacting with a protein residue. Owing to the solvation/desolvation term of GlideScore, this situation was predicted in a few cross-docking situations (e.g., ligand **7** docked into 1HXK protein structure).

When using minimized ligands as input, the ring conformation in the input structure was already different from the crystal structure. This structure optimization stage contributed to a small fraction of the RMSD (<0.3 Å). Compounds in the crystal structures of dGMII were not in their lowest energy conformation but rather in a higher energy conformation induced by environmental constraints in the active site.[32] The effect of the zinc ion and the active site environment on inhibitor distortion has recently been discussed.[69]

Metal ligation

To further evaluate the program's ability to dock the GMII inhibitors, a closer inspection of the poses around the Zn cation was carried out. A clear indication of the predictive power of Glide was given by the computed RMSD's of the metal ligating groups [Fig. 5(b)]. In 54% and 91% of the cases (cross- and self-docking, respectively), the chelating alcohols or diols were positioned within 0.5 and 1.0 Å of the observed positions respectively, even though this docking/scoring method did not account for coordination geometry. AutoDock suffered from the lack of constraints and in a few cases, **8** did not even interact with the zinc cation. The other programs offered the use of constraints to direct the docking and the zinc was chelated is most of the cases. Compounds **1**, **3,** and **5** were generally docked in a binding mode similar to the crystal structure but in a few cases a single alcohol was interacting with the metal, the second alcohol interacting with Asp204, or a different second hydroxyl group was chelating the zinc. Similarly, **2** was often docked with a single alcohol (e.g., O6) interacting with the metal. Interestingly, although the metal chelation was treated as a standard non-bonded interaction in AutoDock, only 5% of the docked structures did not involve the binding of at least one alcohol to the zinc atom. These observations were consistent with our previous report.[47] However, the detailed geometry was not accurately predicted, with only 35% of the ligation being predicted with a deviation of less than 1.0 Å relative to the crystal structure. Surprisingly, even though LigandFit was not among the most accurate docking programs, the metal ligation was fairly well predicted as shown in Figure 5(b). In contrast, FITTED was not very predictive when considering the metal chelation even though overall it ranked second. The lack of a specific metal binding term in the FITTED scoring function may be responsible for this observation.

Overall, Glide clearly outperformed the other programs. As discussed above the apparent poor accuracy of nearly 50% should be taken with great care as most of the compounds were docked properly, the main deviation being attributed to the solvent-exposed moieties. When these moieties were not considered, accuracies higher than 90% were recorded with Glide. The other programs poorly predicted both the metal chelation and the location of the solvent-exposed groups.

Docking to conformational ensembles and flexible proteins

Comparing the self-docking data to the cross-docking data revealed the sensitivity of the seven programs for the protein structure. Figure 7 shows a superposition of 5 of the 10 selected crystal structures. In this figure only the largest side chain moves are shown. For these five residues (Tyr727, Trp95, Arg228, Tyr269, and Asp92), moves of about 1 Å for specific atoms were observed. The location of the zinc atom also varied. Although 1 Å can be seen as negligible, it is roughly the size of an atom and can preclude the proper binding of a func-

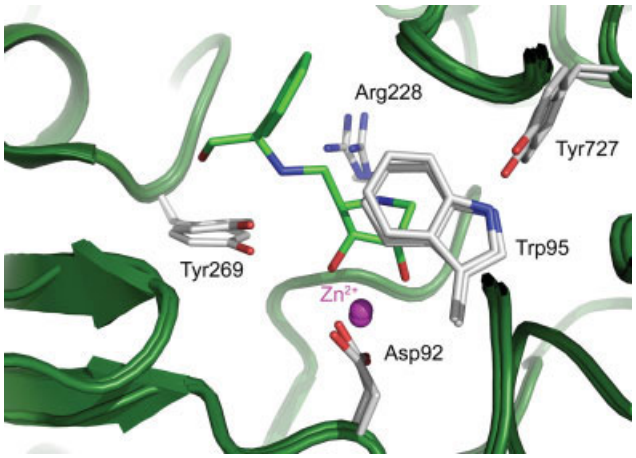

Figure 7

*Superposition of 1HWW, 1HXK, 1R34, 1TQT and 2F18 protein structures (backbone green, side chains grey), and ligand **8** (green). Only selected residues of each structure are shown to illustrate the largest displacements. This figure was generated with PyMOL. [Color figure can be viewed in the online issue, which is available at www.interscience.wiley.com.]*

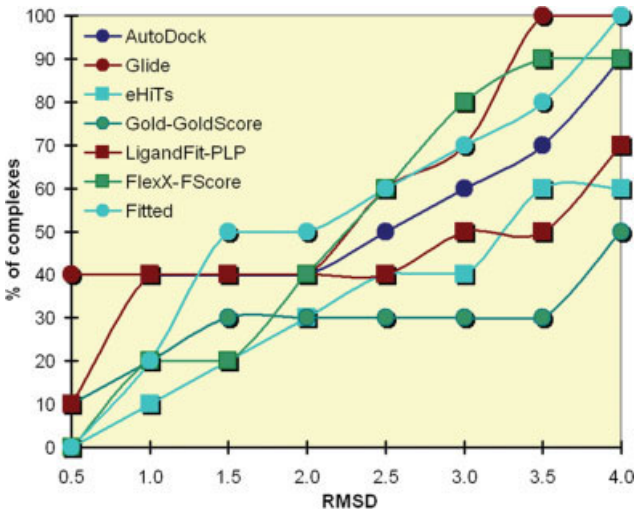

Figure 8

Docking to protein ensembles. Accuracy for the seven programs assessed to dock the 10 ligands to an ensemble of the 10 protein structures, measured as the RMSD between the docked poses and the crystal structure binding mode for all ligand heavy atoms. [Color figure can be viewed in the online issue, which is available at www.interscience.wiley.com.]

tional group of the ligand, significantly affecting the docking accuracy.

The clear dependence of the docking accuracy of ligands (i.e., **7** and **10**) on the protein structure led us to consider docking to flexible proteins. One obvious method was to dock the compounds to the 10 protein structures. Then, the best scoring pose among the 10 docked structures for each inhibitor was considered. Using this approach (docking to multiple conformations), slight to good improvement was observed (Fig. 8). Again, Glide and FITTED appeared as the best two programs. However, these data were collected for only 10 ligands and should not be considered as representative of the overall accuracy of the assessed programs. At low RMSD's (below 1.0 Å), LigandFit/PLP and Glide outperformed the other programs. Their ability to predict the zinc chelation allowed these two programs to very accurately predict the binding mode of the smallest inhibitors.

We next looked at the flexible versions of the programs. An induced-fit docking protocol has recently been made available by Schrödinger.[50] However, the average CPU time required for a single run exceeds 10 h and would therefore be a major limitation to the use of this protocol for drug design. We decided not to include this method in our study. Flexible protein versions of AutoDock[52] and of FlexX, namely FlexE,[51] have been proposed and were used together with FITTED[30] as a complement to the cross-docking studies. However, no significant improvement comparatively to the docking to multiple conformations was observed (data not shown). This indicated that the failures observed were not due to the flexibility of the protein, but to inherent limitations of the docking/scoring methods used by each of the programs evaluated.

Scoring accuracy

When looking at the predicted activities of these weak to strong inhibitors with any of the programs assessed, the scores did not correlate well with the observed activities. The most active swainsonine (**1**) was predicted to be one of the least active inhibitors of the set with all the scoring functions. This revealed that the scoring functions used can accurately discriminate between the different poses, hence predicting reasonable binding modes, but not between compounds of different affinities. In fact, it is well known that the accuracy of current scoring functions for small compounds is still poor,[70,71] with large compounds being often assigned higher scores than small compounds by most of the scoring functions.[72]

Virtual screening using Glide

We next turned our attention to the use of docking-based virtual screening (VS) tool to screen potential α-mannosidase inhibitors. As discussed above, Glide/GlideScore was more accurate in predicting the correct binding mode than any of the other programs assessed. We therefore decided to restrict the VS study to Glide alone, as VS data from a program unable to provide the correct binding mode would be hard to interpret. However, although the overall accuracy of Glide was excellent, the apparent poor accuracy of the scoring function may be a hurdle in virtual screening. To evaluate the performance of Glide for VS, we seeded a library of decoys with previously reported GMII inhibitors and docked the complete library to a single dGMII protein structure. The protein structure from complex 1PS3 was found to be a fair representative (by visual inspection and comparison of active site side chain RMSD) of the set of 10 proteins used in the docking study, hence its selection as the target for the VS. Then, a set of 1000 decoys used by the Schrödinger team to benchmark Glide[55] was seeded with 10 active compounds shown in Table IV. Compound **3** (protein 1PS3 natural ligand) was purposely not selected to prevent biasing self-docking. The activity for some of the compounds was measured on jack bean GMII, a common model for hGMII as discussed in the introduction. At first sight these active compounds **11**–**17**[73–79] can be viewed as poor inhibitors, however low micromolar inhibitors are considered strong inhibitors of GMII.[80,81] In addition, one needs to bear in mind that the primary goal of a VS study is to discover micromolar lead compounds from large libraries and not nanomolar

DOI 10.1002/prot

Table IV
Structures of α-Mannosidase Inhibitors Used for Virtual Screening Evaluation

Compound	IC_{50} (μ*M*)	Inhibitor structure
1	0.017	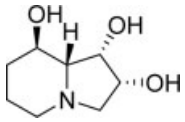
4	70	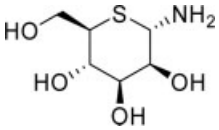
8	80	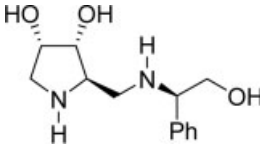
11	0.8[a],73	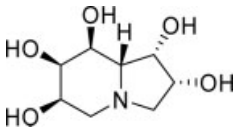
12	9[a],74	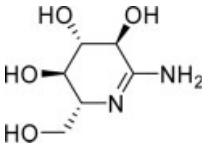
13	10[b],75	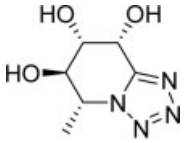
14	12[b],76	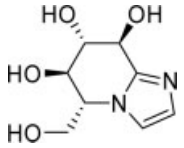
15	0.5[a],77	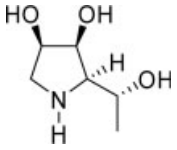
16	40[a],78	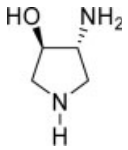
17	20[a],79	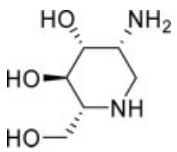

The inhibitory activity is given as IC_{50} on *Drosophila* GMII unless otherwise noted.
[a]K_i on jack bean GMII.
[b]IC_{50} on jack bean GMII.

compounds, which are often developed through lead optimization.

Figure 9 shows the number of known hits retrieved when increasing the fraction of the ranked list. A charge of 1 or 2 (protonated amines) was assigned to each compound and alternate protonation modes were considered. For instance, compound **17** had to be monoprotonated to be able to properly chelate the zinc cation. The tetrazole ring of compound **13** could be protonated at different locations, or not at all, having an estimated pK_a of around 5. The dark blue line in Figure 9 shows the accuracy of docking all the compounds with all the amines protonated and the tetrazole ring of **13** protonated at position 2. The light blue lines represent the results based on the best or worst scores of each compound when considering all the possible protonation states. Obviously, the final score did not take into account the energy required to change the protonation state from the one stable in solution to the one in the protein binding site. As can be seen in Figure 9, half of the active compounds were retrieved in the top 10% regardless of the protonation states selected. However, between 3 and 5 compounds were recovered in the top 2% depending on the chosen protonation states. We noticed that the protonation state was a critical factor to consider, as compounds with two amines (i.e., **1**, **16,** and **17**) provided quite different scores with alternative protonation states.

Overall, this was a very promising result that correlated well with the good performance of Glide in virtual screening studies.[55] Using the same decoy set, Halgren et al. recovered from 50 to 90% of the actives in the top

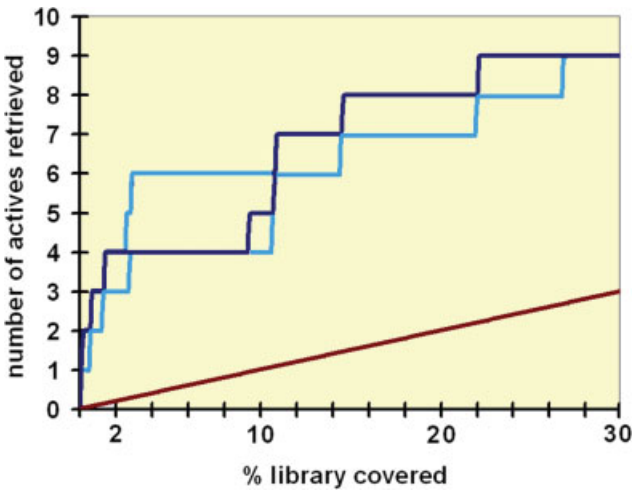

Figure 9
Number of known active compounds recovered as a function of the percentage of the ranked list. Dark blue: standard protonation states, light blue: best and worse scores with various protonation states, brown: random. [Color figure can be viewed in the online issue, which is available at www.interscience.wiley.com.]

Table V
Results for the Virtual Screening of Mannosidase Inhibitors

Compound	Ranking	Score	IC_{50}/K_i (μM)
4	2	−11.99	70
8	3	−10.72	80
14	8	−10.16	12[a]
13	27	−9.94	10[a]
12	15	−9.82	9[a]
17	30	−9.38	20[a]
15	110	−8.25	0.5[a]
11	147	−8.04	0.8[a]
1	222	−7.71	0.017
16	362	−7.22	40[a]

The ranking corresponds to the order of the compound in the sorted list of scores; the score is the GlideScore value of the best docked pose for the compound.
[a]Activity value for jack bean GMII.

10% with most of the proteins studied and less than 50% with p38 MAP kinase. Clearly, Glide is a promising tool for the virtual screening of α-mannosidase inhibitors considering the known poor performance of docking methods with metal-containing proteins. As can be seen in Table V, the most active compounds **1**, **11,** and **15** were assigned lower scores than less active inhibitors, which confirmed the lack of accuracy of GlideScore to rank some of the actives. Nevertheless, having 8 out of 10 seeded actives in the top 15% of the ranked library demonstrated that GlideScore is indeed appropriate for the retrieval of mannosidase inhibitors.

CONCLUSIONS

In medicinal chemistry, crystallography and computational chemistry are well-established tools at the lead generation stage. We have described herein three new three-dimensional structures of *Drosophila melanogaster* Golgi α-mannosidase II:inhibitor complexes and their application to assessing the ability of seven available docking programs to predict the binding mode and binding affinity of α-mannosidase II inhibitors. Overall, Glide outperformed the other docking programs followed by FITTED, GOLD, AutoDock, and FlexX. eHiTS was found to be the least accurate. Unexpectedly, the prediction of the metal coordination geometry appeared to be best with Glide/GlideScore even compared to other programs that included a specific term for metal ligation and coordination geometries.

Although the docked poses were often close to the observed binding modes, the predicted binding constants were not well correlated with the observed inhibition data. The highly active inhibitor swainsonine (**1**) was ranked among the least actives in most of the cases. We believe that metal ligation and solvation were not adequately evaluated in the tested scoring functions, and that large molecules were over-scored. To evaluate the impact of this apparently poor scoring on the performance of Glide, we carried out a VS study and were pleased to obtain enrichment factors in the range observed with nonmetal containing proteins. As previously observed, swainsonine, the most active inhibitor considered, was found to be the outlier of the set with a score much lower than less active inhibitors.

In summary, using Glide, small inhibitors were docked with excellent accuracy (RMSD $<$ 1.1 Å), while larger inhibitors with solvent-exposed polar and nonpolar functional groups were docked with good accuracy (RMSD $\sim$ 2.5 Å). More specifically, the zinc ligation was well predicted in most cases of self and cross-docking, while the largest deviations arose from the solvent-exposed moieties. Finally, we believe that the application of Glide to the VS of large libraries of compounds is a promising strategy for the discovery of novel GMII inhibitors.

ACKNOWLEDGMENTS

We thank Virochem Pharma for a scholarship to CRC. PE was supported by a scholarship from the Canadian Institutes of Health Research (Strategic Training Initiative in Chemical Biology). We thank CLUMEQ (McGill University) and CERMM (Concordia University) for generous allocation of computer resources. Beamtime and technical support provided by APS and CHESS are also gratefully acknowledged.

REFERENCES

1. Dwek RA. Glycobiology: toward understanding the function of sugars. Chem Rev 1996;96:683–720.
2. Kornfeld R, Kornfeld S. Assembly of asparagine-linked oligosaccharides. Annu Rev Biochem 1985;54:631–664.
3. Roth J. Protein *N*-glycosylation along the secretory pathway: relationship to organelle topography and function, protein quality control, and cell interactions. Chem Rev 2002;102:285–303.
4. Herscovics A. Importance of glycosidases in mammalian glycoprotein biosynthesis. Biochim Biophys Acta 1999;1473:96–107.
5. Moremen KW, Trimble RB, Herscovics A. Glycosidases of the asparagine-linked oligosaccharide processing pathway. Glycobiology 1994; 4:113–125.
6. Sears P, Wong CH. Enzyme action in glycoprotein synthesis. Cell Mol Life Sci 1998;54:223–252.
7. Goss PE, Baker MA, Carver JP, Dennis JW. Inhibitors of carbohydrate processing: a new class of anticancer agents. Clin Cancer Res 1995;1:935–944.
8. Dennis JW, Granovsky M, Warren CE. Protein glycosylation in development and disease. Bio Essays 1999;21:412–421.
9. Dennis JW, Granovsky M, Warren CE. Glycoprotein glycosylation and cancer progression. Biochim Biophys Acta 1999;1473:21–34.
10. Couldrey C, Green JE. Metastases: the glycan connection. Breast Cancer Res 2000;2:321–323.
11. Elbein AD, Molyneux RD. Inhibitors of glycoprotein processing. In: Stütz AE, editor. Iminosugars as glycosidase inhibitors. Weinheim: Wiley-VCH; 1999. pp 216–251.
12. Colegate SM, Dorling PR, Huxtable CR. Spectroscopic investigation of swainsonine—alpha-mannosidase inhibitor isolated from Swainsona-Canescens. Aust J Chem 1979;32:2257–2264.
13. Kino T, Inamura N, Nakahara K. Studies of an immunomodulator, swainsonine. II. Effect of swainsonine on mouse immunodeficient system and experimental murine tumor J Antibiot 1985;38:936–940.

DOI 10.1002/prot

14. Goss PE, Reid CL, Bailey D, Dennis JW. Phase IB clinical trial of the oligosaccharide processing inhibitor swainsonine in patients with advanced malignancies. Clin Cancer Res 1997;3:1077–1086.
15. Howard S, Braun C, McCarter J, Moremen KW, Liao YF, Withers SG. Human lysosomal and jack bean α-mannosidases are retaining glycosidases. Biochem Biophys Res Commun 1997;238:896–898.
16. Rabouille C, Kuntz DA, Lockyer A, Watson R, Signorelli T, Rose DR, Van Den Heuvel M, Roberts DB. The Drosophila GMII gene encodes a Golgi α-mannosidase II. J Cell Sci 1999;112:3319–3330.
17. Van den Elsen JMH, Kuntz DA, Rose DR. Structure of Golgi α-mannosidase II: a target for inhibition of growth and metastasis of cancer cells. EMBO J 2001;20:3008–3017.
18. Numao S, Kuntz DA, Withers SG, Rose DR. Insights into the Mechanism of Drosophila melanogaster Golgi α-Mannosidase II through the structural analysis of covalent reaction intermediates. J Biol Chem 2003;278:48074–48083.
19. Rose DR, Kuntz DA, van den Elsen JMH. Crystal structure of drosophila α-mannosidase II and swainsonine complexes its use for identifying mannosidase II activity-modulating ligands and therapeutic applications. US Patent Appl 2002172670, 2002.
20. Cole JC, Murray CW, Nissink JWM, Taylor RD, Taylor R. Comparing protein-ligand docking programs is difficult. Proteins Struct Funct Bioinf 2005;60:325–332.
21. Rester U. Dock around the clock—current status of small molecule docking and scoring. QSAR Comb Sci 2006;25:605–615.
22. Klebe G. Virtual ligand screening: strategies, perspectives and limitations. Drug Discov Today 2006;11:580–594.
23. Cavasotto CN, Orry AJW, Abagyan RA. The challenge of considering receptor flexibility in ligand docking and virtual screening. Curr Comput-Aided Drug Des 2005;1:423–440.
24. Friesner RA, Knoll EH, Banks JL, Murphy RB, Halgren TA, Klicic JJ, Mainz DT, Repasky MP, Shaw DE, Shenkin PS, Shelley M, Perry JK, Francis P. Glide: a new approach for rapid, accurate docking and scoring, Part 1. Method and assessment of docking accuracy. J Med Chem 2004;47:1739–1749.
25. Jones G, Willett P, Glen RC, Leach AR, Taylor R. Development and validation of a genetic algorithm for flexible docking. J Mol Biol 1997;267:727–748.
26. Rarey M, Kramer B, Lengauer T, Klebe G. A fast flexible docking method using an incremental construction algorithm. J Mol Biol 1996;261:470–489.
27. Venkatachalam CM, Jiang X, Oldfield T, Waldman M. LigandFit: a novel method for the shape-directed rapid docking of ligands to protein active sites. J Mol Graphics Model 2003;21:289–307.
28. Zsoldos Z, Szabo I, Szabo Z, Johnson AP. Software tools for structure based rational drug design. J Mol Struct: THEOCHEM 2003; 666/667:659–665.
29. Morris GM, Goodsell DS, Huey R, Olson AJ, Halliday RS, Hart WE, Belew RK. Automated docking using a Lamarckian genetic algorithm and an empirical binding free energy function. J Comput Chem 1998;19:1639–1662.
30. Corbeil CR, Englebienne P, Moitessier N. Docking ligands into flexible and solvated macromolecules, Part 1. Development and validation of FITTED 1.0. J Chem Inf Model 2007;47:435–439.
31. Kuntz DA, Ghavami A, Johnston BD, Pinto BM, Rose DR. Crystallographic analysis of the interactions of Drosophila melanogaster Golgi α-mannosidase II with the naturally occurring glycomimetic salacinol and its analogues. Tetrahedron: Asymmetry 2005;16:25–32.
32. Shah N, Kuntz DA, Rose DR. Comparison of kifunensine and 1-deoxymannojirimycin binding to class I and II a-mannosidases demonstrates different saccharide distortions in inverting and retaining catalytic mechanisms. Biochemistry 2003;42:13812–13816.
33. Maestro. 7.0. Portland, OR: Schrödinger, LLC; 2004.
34. Jaguar. 6.0. Portland, OR: Schrödinger, LLC; 2004.
35. Tiraboschi G, Gresh N, Giessner-Prettre C, Pedersen LG, Deerfield DW. Parallel ab initio and molecular mechanics investigation of polycoordinated Zn(II) complexes with model hard and soft ligands: variations of binding energy and of its components with number and charges of ligands. J Comput Chem 2000;21:1011–1039.
36. Sybyl. 7.0. St. Louis, MO: Tripos, Inc.; 2005.
37. Gasteiger J, Marsili M. Iterative partial equalization of orbital electronegativity—a rapid access to atomic charges. Tetrahedron 1980; 36:3219–3228.
38. Cerius2. 4.10. San Diego, CA: Accelrys, Inc.; 2005.
39. Berman HM, Westbrook J, Feng Z, Gilliland G, Bhat TN, Weissig H, Bourne PE, Shindyalov IN. The protein data bank. Nucleic Acids Res 2000;28:235–242.
40. Kavlekar LM, Kuntz DA, Wen X, Johnston BD, Svensson B, Rose DR, Pinto BM. 5-Thio-D-glycopyranosylamines and their amidinium salts as potential transition-state mimics of glycosyl hydrolases: synthesis, enzyme inhibitory activities, X-ray crystallography, and molecular modeling. Tetrahedron: Asymmetry 2005;16:1035–1046.
41. Popowycz F, Gerber-Lemaire S, Rodriguez-García E, Schütz C, Vogel P. Synthesis and α-mannosidase inhibitory evaluation of (2R,3R,4S)- and (2S,3R,4S)-2-(aminomethyl)pyrrolidine-3,4-diol derivatives. Helv Chim Acta 2003;86:1914–1948.
42. Popowycz F, Gerber-Lemaire S, Schütz C, Vogel P. Syntheses and glycosidase inhibitory activities of 2-(Aminomethyl)-5-(hydroxymethyl)pyrrolidine-3,4-diol derivatives. Helv Chim Acta 2004;87:800–810.
43. Fiaux H, Popowycz F, Favre S, Schütz C, Vogel P, Gerber-Lemaire S, Juillerat-Jeanneret L. Functionalized pyrrolidines inhibit ?-mannosidase activity and growth of human glioblastoma and melanoma cells. J Med Chem 2005;48:4237–4246.
44. Moitessier N, Westhof E, Hanessian S. Docking of aminoglycosides to hydrated and flexible RNA. J Med Chem 2006;49:1023–1033.
45. Hoops SC, Anderson KW, Merz Jr KM. Force field design for metalloproteins. J Am Chem Soc 1991;113:8262–8270.
46. Kellenberger E, Rodrigo J, Muller P, Rognan D. Comparative evaluation of eight docking tools for docking and virtual screening accuracy. Proteins 2004;57:225–242.
47. Hanessian S, Moitessier N, Therrien E. A comparative docking study and the design of potentially selective MMP inhibitors. J Comput-Aided Mol Des 2001;15:873–881.
48. Hanessian S, MacKay DB, Moitessier N. Design and synthesis of matrix metalloproteinase inhibitors guided by molecular modeling. Picking the S1 pocket using conformationally constrained inhibitors. J Med Chem 2001;44:3074.
49. Kerwin SM. Computer Software Review: eHiTS 5.1.6, SimBioSys Inc. J Am Chem Soc 2005;127:8899–8900.
50. Sherman W, Day T, Jacobson MP, Friesner RA, Farid R. Novel procedure for modeling ligand/receptor induced fit effects. J Med Chem 2006;49:534–553.
51. Claußen H, Buning C, Rarey M, Lengauer T. FlexE: efficient molecular docking considering protein structure variations. J Mol Biol 2001;308:377–395.
52. Österberg F, Morris GM, Sanner MF, Olson AJ, Goodsell DS. Automated docking to multiple target structures: incorporation of protein mobility and structural water heterogeneity in autodock. Proteins 2002;46:34–40.
53. Moitessier N, Therrien E, Hanessian S. A method for induced-fit docking, scoring, and ranking of flexible ligands. Application to peptidic and pseudopeptidic β-secretase (BACE 1) inhibitors. J Med Chem 2006;49:5885–5894.
54. Glide. 3.5. Portland, OR: Schrödinger, LLC; 2004.
55. Halgren TA, Murphy RB, Friesner RA, Beard HS, Frye LL, Pollard WT, Banks JL. Glide: a new approach for rapid, accurate docking and scoring. 2 enrichment factors in database screening J Med Chem 2004;47:1750–1759.
56. Eldridge MD, Murray CW, Auton TR, Paolini GV, Mee RP. Empirical scoring functions. I. The development of a fast empirical scoring

function to estimate the binding affinity of ligands in receptor complexes. J Comput Aided Mol Des 1997;11:425–445.
57. FlexX. 1.13. Sankt Augustin, Germany: BioSolveIT; 2003.
58. Kramer B, Rarey M, Lengauer T. Evaluation of the FlexX incremental construction algorithm for protein-ligand docking. Proteins 1999; 37:228–241.
59. Rarey M, Kramer B, Lengauer T. Multiple automatic base selection: protein-ligand docking based on incremental construction without manual intervention. J Comput Aided Mol Des 1997;11:369–384.
60. Hindle SA, Rarey M, Buning C, Lengauer T. Flexible docking under pharmacophore type constraints. J Comput-Aided Mol Des 2002; 16:129–149.
61. AutoDock. 3.0. La Jolla, CA: The Scripps Research Institute; 1998.
62. AutoDock 4 beta release. http://autodock.scripps.edu/news_files/autodock-4-beta-release (accessed Jan 25, 2007).
63. GOLD. 3.0. Cambridge, UK: CCDC; 2005.
64. eHiTS. 5.1. Toronto, ON, Canada: SimBioSys; 2005.
65. For more information see: http://www.simbiosys.ca/ehits/ehits_newfeatures.html (accessed Jan 25, 2007).
66. Fletcher R, Reeves CM. Function minimization by conjugate gradients. Comp J 1964;7:149–154.
67. Kuntz ID, Blaney JM, Oatley SJ, Langridge R, Ferrin TE. A geometric approach to macromolecule-ligand interactions. J Mol Biol 1982;161:269–288.
68. Muegge I, Martin YC. A general and fast scoring function for protein-ligand interactions: a simplified potential approach. J Med Chem 1999;42:791–804.
69. Kuntz DA, Liu H, Bols M, Rose DR. The role of the active site Zn in the catalytic mechanism of the GH38 Golgi α-mannosidase II: implications from neuromycin inhibition. Biocatal Biotransform 2006;24:55–61.
70. Wang R, Lu Y, Wang S. Comparative evaluation of 11 scoring functions for molecular docking. J Med Chem 2003;46:2287–2303.
71. Ferrara P, Gohlke H, Price DJ, Brooks CL, III, Klebe G. Assessing scoring functions for protein-ligand interactions. J Med Chem 2004;47:3032–3047.
72. Jacobsson M, Karlén A. Ligand bias of scoring functions in structure-based virtual screening. J Chem Inf Model 2006;46:1334–1343.
73. Picasso S, Chen Y, Vogel P. Glycosidase inhibition by 1,5-dideoxy-1,5-iminooctitols and 1,2,6,7,8-pentahydroxyindolizidines. Carbohydrate Lett 1994;57:1–8.
74. Papandreou G, Tong MK, Ganem B. Amidine, amidrazone, and amidoxime derivatives of monosaccharide aldonolactams: synthesis and evaluation as glycosidase inhibitors. J Am Chem Soc 1993;115:11682–11690.
75. Davis BG, Brandstetter TW, Hackett L, Winchester BG, Nash RJ, Watson AA, Griffiths RC, Smith C, Fleet GWJ. Tetrazoles of manno- and rhamno-pyranoses: contrasting inhibition of mannosidases by [4.3.0] but of rhamnosidase by [3.3.0] bicyclic tetrazoles. Tetrahedron 1999;55:4489–4500.
76. Tatsuta K, Mijura S, Ohta S, Gunji I. Syntheses and glycosidase inhibiting activities of nagstatin analogs [2]. J Antibiot 1995;48:286–288.
77. Eis MJ, Rule CJ, Wurzburg BA, Ganem B. Synthesis of 1,4,6-trideoxy-1,4-imino-D-mannitol: a potentα-mannosidase inhibitor. Tetrahedron Lett 1985;26:5397–5398.
78. Limberg G, Lundt I, Zavilla J. Deoxyiminoalditols from aldonic acids VI. Preparation of the four stereoisomeric 4-amino-3-hydroxypyrrolidi nes from bromodeoxytetronic acids. Discovery of a new α-mannosidase inhibitor. Synthesis 1999:178–183.
79. Le Merrer Y, Poitout L, Depezay JC, Dosbaa I, Geoffroy S, Foglietti MJ. Synthesis of azasugars as potent inhibitors of glycosidases. Bioorg Med Chem 1997;5:519–533.
80. Asano N, Nash RJ, Molyneux RJ, Fleet GWJ. Sugar-mimic glycosidase inhibitors: natural occurrence, biological activity and prospects for therapeutic application. Tetrahedron: Asymmetry 2000;11:1645–1680.
81. Ganem B. Inhibitors of carbohydrate-processing enzymes: design and synthesis of sugar-shaped heterocycles. Acc Chem Res 1996; 29:340–347.

 DOI 10.1002/prot